SPRING LOADED: USING LOAD RECONSTRUCTION FOR RUBBER FATIGUE ON A POGO STICK DIGITAL TWIN

Will Mars, Ph.D.
President, Endurica

Tim Hunter, Ph.D.
President, Wolf Star Technologies, LLC

SUMMARY

Digital Twin applications that integrate in-situ load measurements with periodically updated simulations of remaining fatigue life hold great promise for creating huge value in maintenance and logistical operations. In this work, the authors implement two commercially available, off-the-shelf solutions to create a closed loop pogo stick digital twin that tracks damage accumulation due to actual loads experienced. A pogo stick was chosen because it experiences highly non-linear loading. The system records 12 strain gauges on the pogo stick frame at 1000 Hz. Strain gauges were placed using the True-Load load reconstruction. The True-Load process automatically creates strain correlation plots comparing measured strain to the strains in the FEA model simulated by the reconstructed loads. It also converts the strain gauge signals into 3 mutually perpendicular load channels that then are fed to a simulation of the pogo stick's rubber tip. After each "operating" session, load history from the pogo stick is downloaded and accumulated as fatigue damage in a digital twin that tracks the remaining life of the rubber tip of the pogo stick. In order to accelerate loads processing to real-time speeds, the Endurica EIE interpolation engine has been used. EIE uses pre-computed finite element solutions of the rubber tip of the pogo stick under a series of load cases to rapidly convert input load history into strain tensor component history for each finite element. The Endurica DT incremental fatigue solver is then used to accumulate damage in all finite elements of the model, for each operating session. The result is a continually updated account of remaining life left in the pogo stick tip due to actual loads experienced. Whether you are developing a new product, or operating a digital twin, combining real-time high accuracy structural loads with real-time fatigue evaluation software will propel you leaps and bounds towards a digital twin for durability.

SPRING LOADED: USING LOAD RECONSTRUCTION FOR RUBBER FATIGUE ON A POGO STICK DIGITAL TWIN

Nomenclature:			
FEA	Finite Element Analysis	F	Applied Force
ε	Strain	I	Identity matrix
$\varepsilon_{i,j}$	Strain response from load i at location j	T	Energy release rate
C	Correlation Matrix	$r(T)$	Fatigue crack growth rate law
c_0, c_f	Initial and final crack length	N_f	Fatigue life

1 Digital Twins

With the Internet of Things (IoT), the advent of ubiquitous computing and networking infrastructure, along with inexpensive and reliable measurement technology has opened opportunities to deliver unprecedented levels of real-time integration between physical structures and their virtual representations. Digital Twin applications are especially promising. A Digital Twin provides up to date, detailed analytics on the state and history of an asset/structure. Such analytics are valuable for maintenance and logistical operations, where unpredictable failures can be mitigated and eliminated by tracking damage accumulation under the history of actual loads.

Two barriers to the implementation of such a Digital Twin have been 1) the ability to measure in-situ the history of all load inputs to a structure, and 2) the time required for executing structural and fatigue analyses. In addition, traditional Digital Twins are open loop. An open loop digital twin receives input from a measurement and plays back previously calculated simulations via a look up table or state space map. The problem with this approach is that if the physical structure changes, the Digital Twin will perform erroneous calculations. Presented here is a closed loop structural Digital Twin. As part of the load calculation from measured strain data, the True-Load software creates real-time correlation plots between measured strain and simulated strain. This way, the loads can be used with confidence in the downstream Endurica durability analysis.

2 Problem Statement

The goal of this project is to provide real-time, up-to-date views of damage distribution accumulated in the rubber tip of a pogo stick.

3 High Level Workflow: Load Reconstruction → Rubber Fatigue

At the macro level, the process for calculating the durability of the rubber component with Endurica begins with load measurement. With the complex structure of the Pogo Stick, the in-situ technique of measuring loads using True-Load was deployed. Figure 3-1 shows a schematic of this process. The first step is to apply unit load cases to an FEA model. Once the response to these unit loads are calculated, the True-Load software identifies the location for placing strain gauges. This strain gauge placement will guarantee that the loading from measured strains can be back calculated. Once the strain gauge locations are identified, the physical structure is then instrumented with strain gauges. Strains are collected during operation. These measured strains are then used to calculate the loads on the structure using the True-Load software. Once the loads are calculated, the loads are passed over to the Endurica software for durability analysis.

Using a set of pre-computed finite element solutions, the received loads are used by Endurica EIE to rapidly generate corresponding strain histories for each finite element in a model of the rubber tip. The strain histories are then fed to the Endurica DT incremental fatigue solver to compute the damage accrued in the rubber tip in each element. Damage accrual is tracked in two ways. First, through the effect on crack growth. Second, through the effect on computed residual life. After processing each new set of loads, the results are presented on a dashboard so that the user can track the remaining fatigue life in the rubber tip. This process is repeated each time a new set of load measurements becomes available.

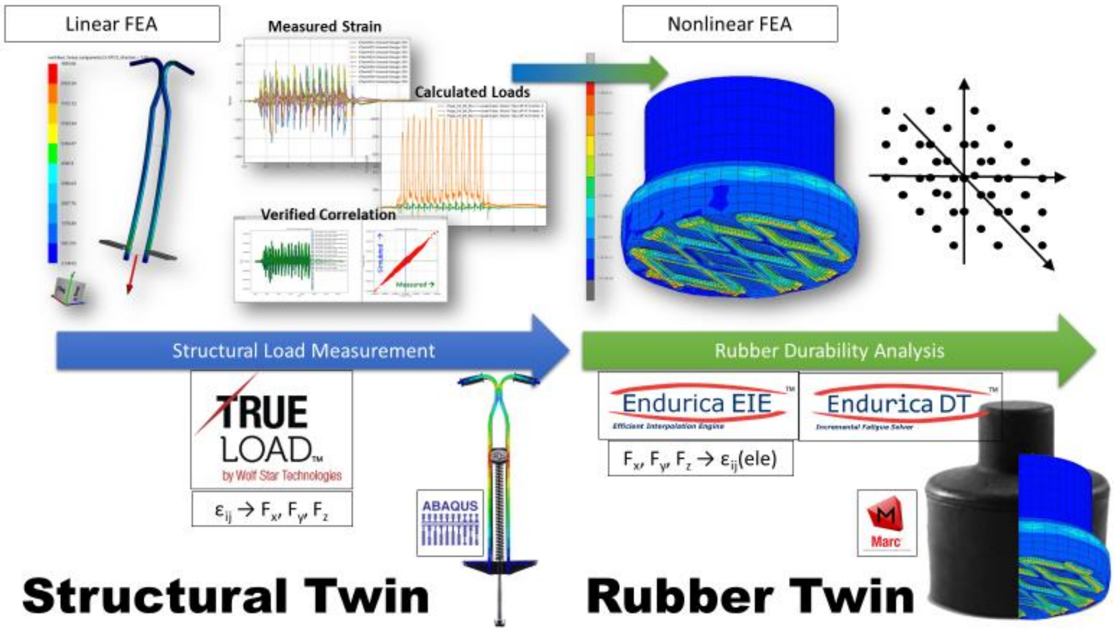

Figure 3-1 High Level Workflow

4 Load Reconstruction: True-Load

4.1 Introduction

The following introduction is excerpted from a paper co-authored by this author which is sited in reference [9] with minor modifications.

A structure responds to external loads (or moments) imposed on it with changes in quantities, such as stresses and strains, displacements, kinematic deformations, etc. This paper addresses the problem of measurement of time varying loads acting on a component utilizing direct strain measurement on the structure. A linear relationship between the measured strains and the applied loads is created. The relationship, i.e., the transfer function between the applied loads and the measured quantity, can be established numerically (e.g., using finite elements), mathematically, or experimentally.

Kinematic response measurements using displacement transducers and accelerometers are well established and well documented [1]. An alternative approach involves measurement of strains using strain gauges [2]. The need to measure strains, stresses or other physical quantities is apparent since these are the ultimate concern of a designer interested in ensuring structural safety. Furthermore, since the gauges are relatively inexpensive, the use of strain gauges to measure dynamic forces acting on a structure has become quite popular in structural dynamics testing [2–6]. In these works, both the normal displacement modes and the strain modes are used to describe dynamic characteristics of the structure.

While the concept of modal strain was used in the mid-1980s to describe dynamic behaviour of a structure, it was not until 1989 when Bernasconi and Ewins [3] presented a sound theoretical basis of modal stress/strain fields. The relationship between strain frequency response function and displacement frequency response function has also been explored by several authors [4–6]. While both the strain and displacement modes are intrinsic dynamic characteristics of a structure and correspond to each other, it has been noted in [6] that for sensitivity reasons, strain modal analysis is more useful in dynamic design of structures with features such as holes, grooves and cracks.

To illustrate the use of strain gauges for recovery of dynamic loads, many of the works mentioned above considered a simply supported cantilevered beam on which gauges were located in an ad hoc manner. While the gauge location on a straight cantilevered beam may be intuitive under certain loading conditions, the same cannot be said of a complex structure where a trial-and-error approach to gauge placement can result in poor load estimates. This is because the gauge may be placed at a location where it has a relatively low sensitivity to the load(s) to be estimated. Further, for multidegree of freedom force gauges, the cross-sensitivity [7] between the gauges may not be small. As a result, the strain data obtained from many of the gauges may be of little use, and the load estimates may not be precisely known.

For static loads, the influence of gauge locations and orientations on the quality of load estimates is discussed in [8]. However, in this work, it was noted that an analysis of all possible combinations of gauge placements would be too time-consuming for most problems. Consequently, only a few ad hoc groups of gauges were selected for analysis. If all possible gauge locations and orientations are not analysed, the results are not guaranteed to be optimal, which in turn, may not yield the best possible load estimates.

To overcome the shortcomings mentioned above, Dhingra, et al [9] outlines an approach for formulating and solving the gauge placement problem when the imposed loads being estimated induce vibrations in the structure, resulting in time varying dynamic strains. The accuracy of load estimates is dependent on the placement (location and orientation) of the strain gauges, and the number of strain modes retained in the analysis. A sequential exchange algorithm based approach [12,13] is used to select the optimum locations, and angular orientations of the strain gauges. This paper presents the application of this technique to a pogo stick complete with experimental measurements and comparison of simulated results to measured quantities.

4.2 True-Load Load Reconstruction Mathematical Foundation

Load reconstruction works on structures that behave linearly during the event of interest. The structure can undergo non-linear behaviour prior to or after the event of interest. The term linear in this context means that the strain response is proportional to the applied loading. Portions of the structure may behave non-linearly. For example, local yielding near welds, bolted joints or boundary conditions may undergo non-linear strain response. Load reconstruction will continue to be effective if the nominal portions of the structure undergo linear response to the applied loading. Structures with gross yielding will not be appropriate for load reconstruction. Schematically, the concept of linearity can be illustrated as follows:

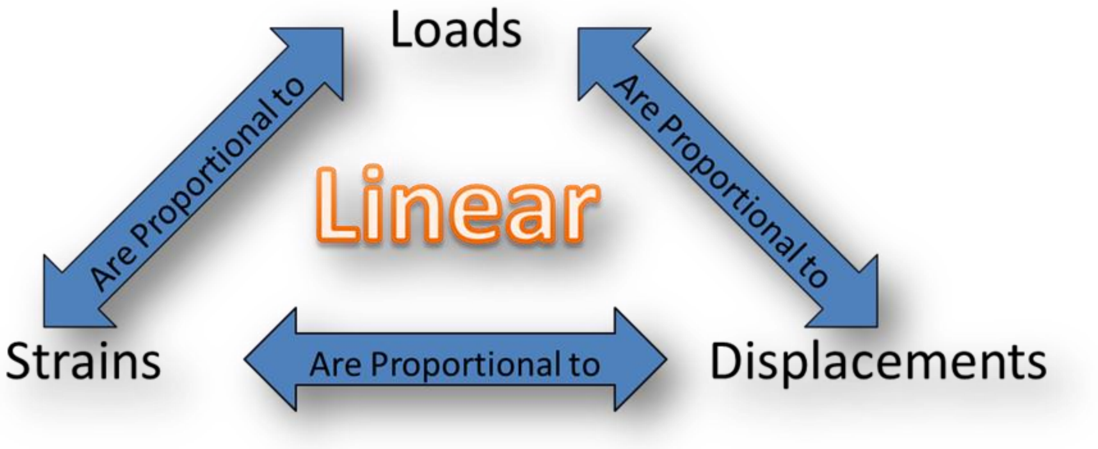

Figure 4-1 Linear material behaviour schematic

This linear relationship can be represented mathematically as follows:

$$F = Kx$$

Equation 1: Hooke's Law

and

$$\varepsilon C = F$$

Equation 2: Influence Coefficient Equation

Constructing a relationship for the strain equation that would work with fixed strain locations (e.g. gauges) and a series of loads cases will yield:

$$\begin{bmatrix} \varepsilon_{1,1} & \varepsilon_{1,2} & \vdots & \varepsilon_{1,m} \\ \varepsilon_{2,1} & \varepsilon_{2,2} & \vdots & \varepsilon_{2,m} \\ \cdots & \cdots & \ddots & \vdots \\ \varepsilon_{n,1} & \varepsilon_{n,2} & \cdots & \varepsilon_{n,m} \end{bmatrix} [C_{m\,x\,n}] = \begin{bmatrix} F_1 & 0 & 0 & 0 \\ 0 & F_2 & 0 & 0 \\ 0 & 0 & \ddots & 0 \\ 0 & 0 & 0 & F_n \end{bmatrix}$$

Equation 3: Influence Coefficient Equation Matrix Form

In the above equation the strain matrix [ε] has dimensions of n loads by m gauges. The load matrix [F] on the right-hand side has dimensions of n loads by n loads. The matrix of proportionality [C] then must have dimensions of m gauges by n loads.

Each row in the strain matrix represents the strain values at a set of specific locations and orientations in the FEA model. The values in each row represent the strain response due to the corresponding load case. The columns of the strain matrix represent individual uniaxial gauge strain response. In the construct presented above, the loading matrix has been diagonalized. In general, this is not necessary, but for the developments presented here, it is convenient. Furthermore, the diagonal entries in the force matrix represent scalar multiples of the corresponding load cases. For our purposes we will set the scalar multiples to unity. This will then yield:

$$\begin{bmatrix} \varepsilon_{1,1} & \varepsilon_{1,2} & \vdots & \varepsilon_{1,m} \\ \varepsilon_{2,1} & \varepsilon_{2,2} & \vdots & \varepsilon_{2,m} \\ \cdots & \cdots & \ddots & \vdots \\ \varepsilon_{n,1} & \varepsilon_{n,2} & \cdots & \varepsilon_{n,m} \end{bmatrix} [C_{m\,x\,n}] = [I]$$

Equation 4: Influence Coefficient Equation set to Unity

Then to solve for C, a simple pseudo inverse needs to be constructed

$$[C] = [\varepsilon^T \varepsilon]^{-1} \varepsilon^T$$

Equation 5: Correlation Matrix

The matrix C exists for a very large possible choices for strain gauge locations. The C matrix is optimal and most stable when the determinant of the self-projected strain matrix is maximum. A sequential exchange search algorithm is deployed that looks for the gauge locations that maximize this determinant.

Once the C matrix is calculated, loading profiles can be back calculated. Given vectors of strains collected from the test structure, the loads can simply be calculated via:

$$\begin{bmatrix} \varepsilon_{t_1,1} & \varepsilon_{t_1,2} & \vdots & \varepsilon_{t_1,m} \\ \varepsilon_{t_2,1} & \varepsilon_{t_2,2} & \vdots & \varepsilon_{t_2,m} \\ \cdots & \cdots & \ddots & \vdots \\ \varepsilon_{t_{end},1} & \varepsilon_{t_{end},2} & \cdots & \varepsilon_{t_{end},m} \end{bmatrix} [C_{m\,x\,n}] = \begin{bmatrix} F_{1_{t_1}} & F_{2_{t_1}} & \cdots & F_{n_{t_1}} \\ F_{1_{t_2}} & F_{2_{t_2}} & \cdots & F_{n_{t_2}} \\ \vdots & \vdots & \vdots & \vdots \\ F_{1_{t_{end}}} & F_{2_{t_{end}}} & \cdots & F_{n_{t_{end}}} \end{bmatrix}$$

Equation 6: Time domain expansion of Forces

The strain matrix on the left-hand side of the above equation represents strain gauge values (columns) at each point of time of data collection (rows). This is the strain data that has been collected from a test event. The right-hand side of the equations represents a set of vectors for scaling each load case. If the individual load cases are scaled by each vector and the results are linearly superimposed, then the resulting strains at the gauge locations at the corresponding row in the test strain matrix are guaranteed to match. Furthermore, any other response in the structure that is behaving linearly will be available through this superposition.

4.3 Load Reconstruction Solution Procedure

Summarized next are the steps involved in the recovery of dynamic loads acting on a component which has a finite number of strain gauges located on the component to measure time varying strains.

Create a series of unit load cases on the FEA model that represent locations and directions of loads applied to the structure. These loads are unit loads (e.g. 1KN) and should be designed such that if they were linearly superimposed on the structure, they could approximate the operating loads. Solve the FEA model for the unit loads constructed in this step.

Search the structure for optimal strain gauge placement using the technique referred to in the introduction. Store the correlation matrix to disc. For the purposes of this paper, this was accomplished using Wolf Star Technologies' True-Load/Pre-Test software.

Place the strain gauges on the physical part and measure time histories of strain in operation.

Calculate the time varying loads using Equation 6.

This process can be summarized with the following diagram:

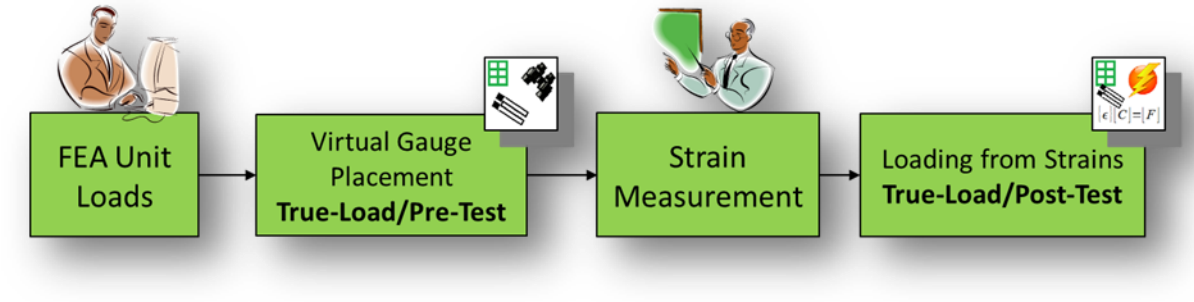

Figure 4-2 Load Reconstruction Process Schematic

4.4 The Pogo Stick Loading Problem

Figure 4-3 Pogo Stick being tested

This exercise will recover the loading on a Pogo Stick. The Flybar™ Super Pogo Stick was purchased from Amazon. The 3D model of the pogo stick was reverse engineered. The instrumentation work was performed by Wolf Star Technologies' Senior Application Engineer, Cynde Murphy.

Figure 4-4 DTS Slice Micro DAQ

The DAQ system being used is a 12 channel DTS Slice Micro DAQ. The unit is powered by a small battery. Data is downloaded via USB cable. The strain gauges used were Micro Measurements CEA-XX-250UW-350-P2 strain gauges. These gauges are 0.250 inch gauge length gauges with pre-soldered lead wires. The lead wires are unshielded. The lead wires were trimmed short and attached to the shielded cabling of the DAQ system to minimize external electronic noise.

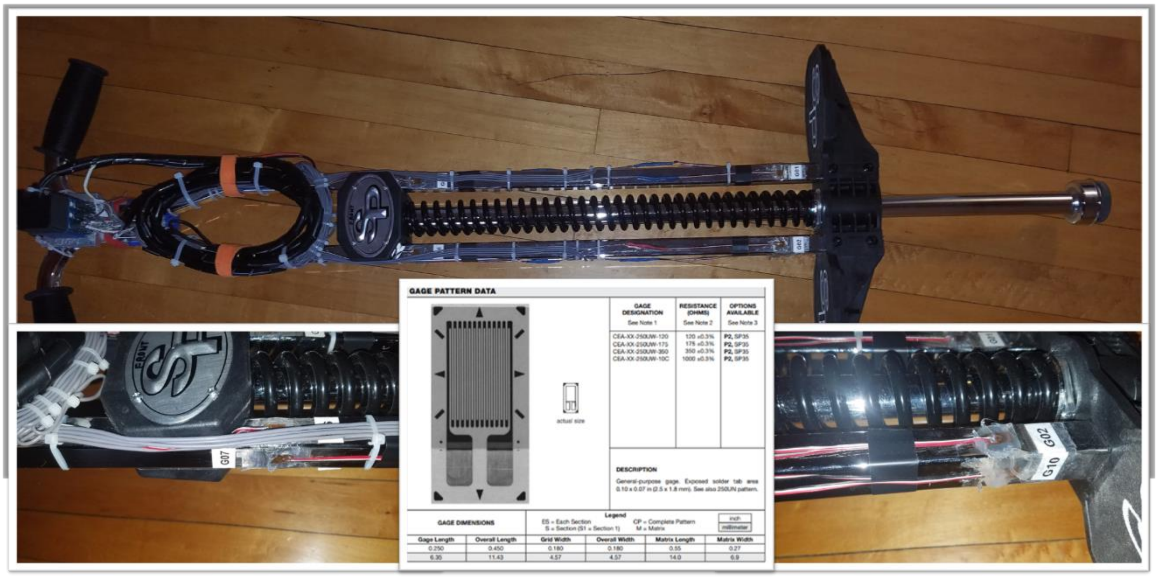

Figure 4-5 Strain Gauge Placement

4.5 The Pogo Stick: Unit Loads

The unit loads for the Pogo Stick are created in an FEA model. Where the top of spring reacts into the Pogo Stick structure, three unit loads (FX, FY, FZ) were placed to simulate the spring loading. At the footboard support crossbar, three moments (MX, MY, MZ) were placed to simulate inputs coming into the structure from the footboards.

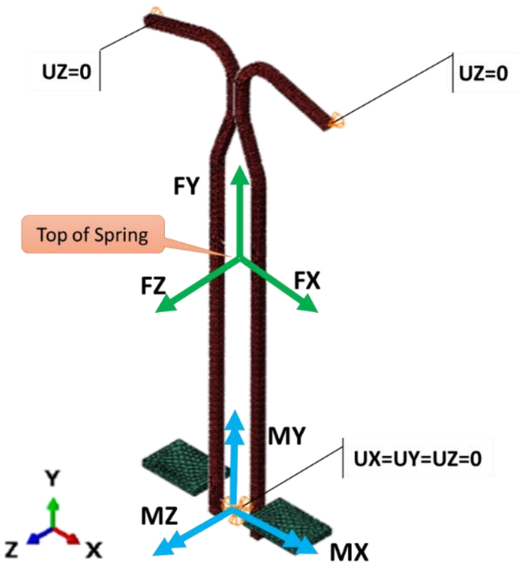

Figure 4-6 FEA Unit Loads

The footboard support crossbar was fixed in 3DOF. The ends of the handlebars were restrained in the Z direction.

The Pogo Stick: Pre-Test

The True-Load/Pre-Test software was used to load in the six unit load cases and the corresponding strain results from the FEA model. The GUI from the True-Load software is shown below with the table of the unit load cases loaded.

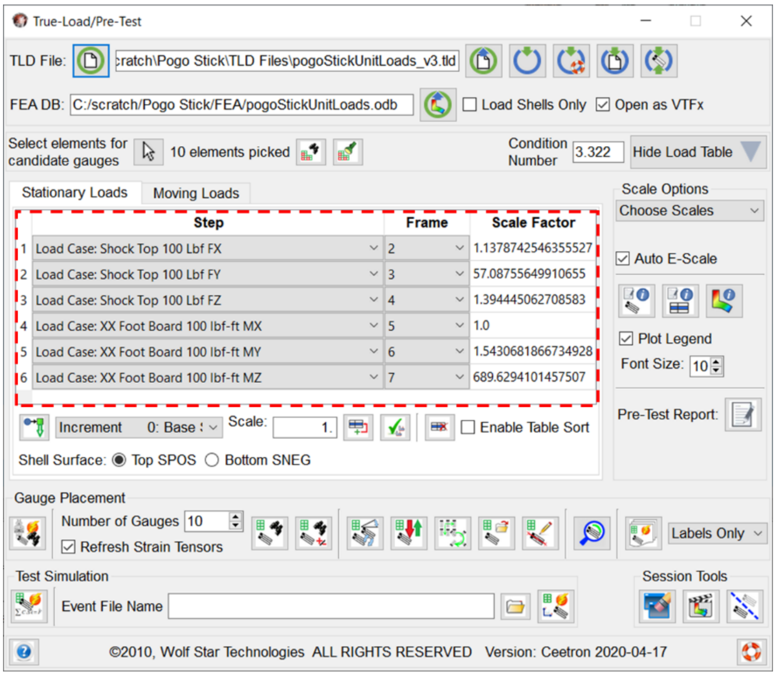

Figure 4-7 Pre-Test GUI with Load Table

The final strain gauge placement is shown below.

Figure 4-8 Virtual Strain Gauge Placement

An important phenomena to understand is the stability of the correlation matrix. The True-Load software provides a utility that calcuates the ideal strain for each unit load case and then applies a 5% random signal noise to the idealized strain. These strain signals are then multiplied by the correlation matrix to determine the correpsonding load response. Ideally, each load should be turned on one by one and the other loads would be turned off. The plot below shows the load sensitivty to strain noise for this configuration of gauges.

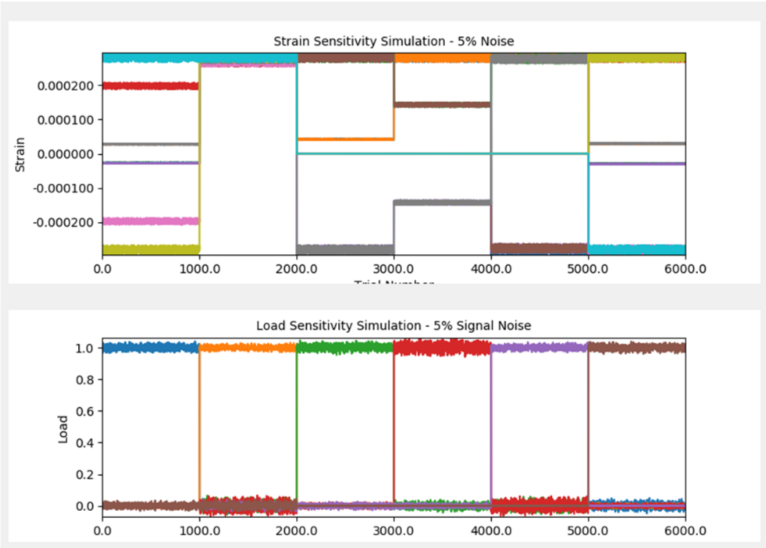

Figure 4-9 Load Sensitivity to Strain Signal Noise

This plot shows that the system of gauges chosen produces a very stable system of load reconstruction which can tolerate noise in the strain signals.

4.6 The Pogo Stick: Strain Gauge Application

A series of drawings were created which located the strain gauges on the physical structure. These drawings were then used to place the gauges on the physical part using callipers and other measurement techniques.

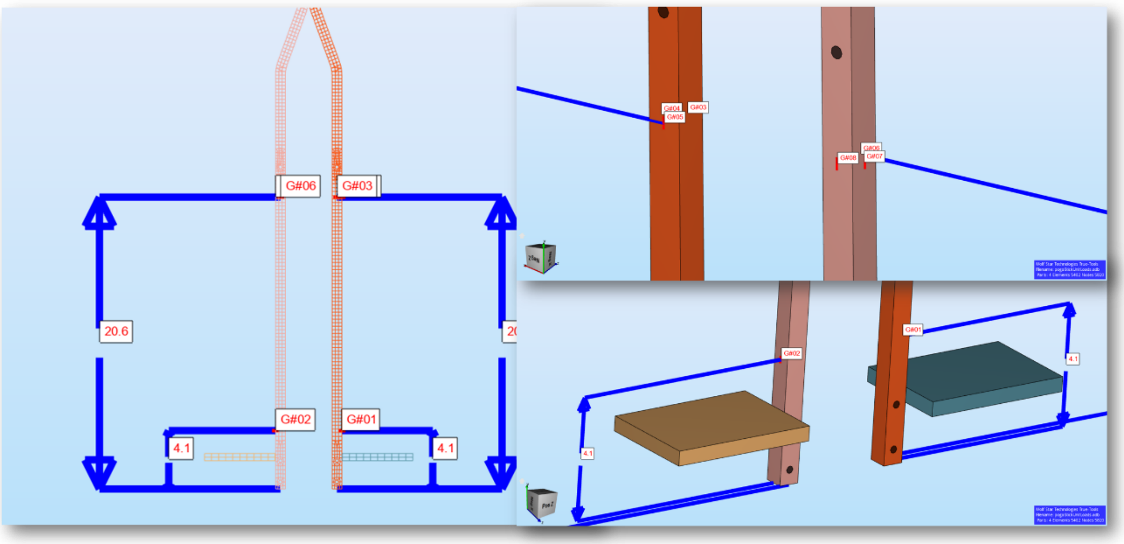

Figure 4-10 Strain Gauge Installation

4.7 Pogo Stick: Test Data Collection

Once the scooter was fully instrumented, the strain gauges were connected to a DTS Slice Micro DAQ system. The strain data was sampled at 1000 samples per second.

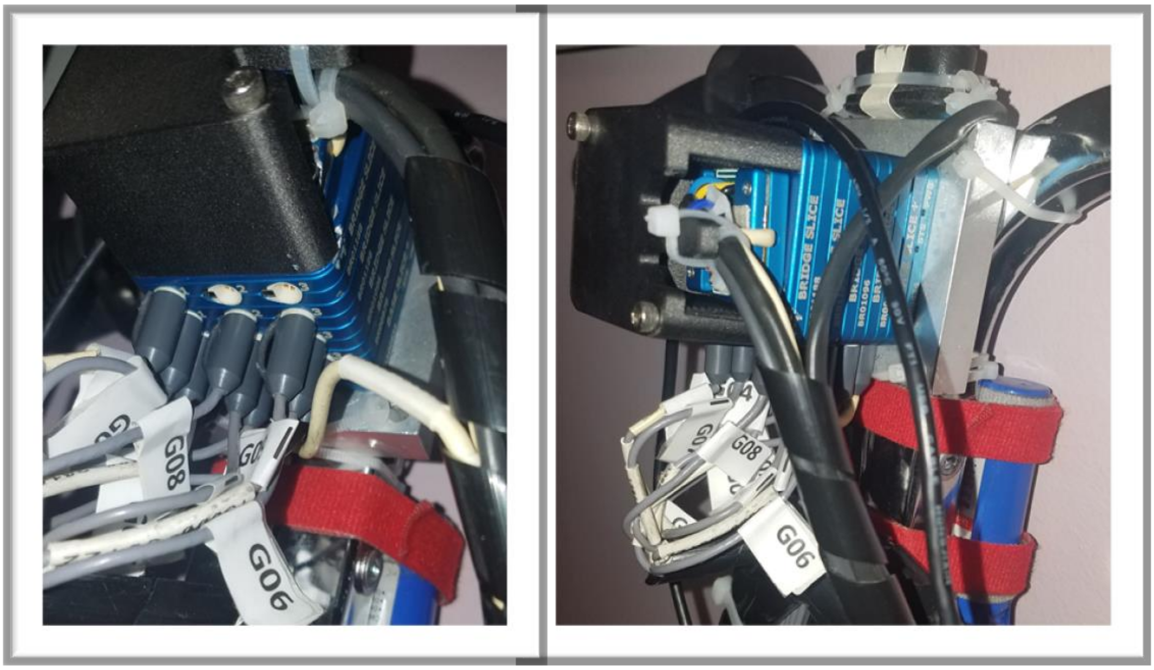

Figure 4-11 DAQ used for Strain Data Collection

The data collection was performed under normal operation on a variety of surfaces. A typical trace of strain data is shown below.

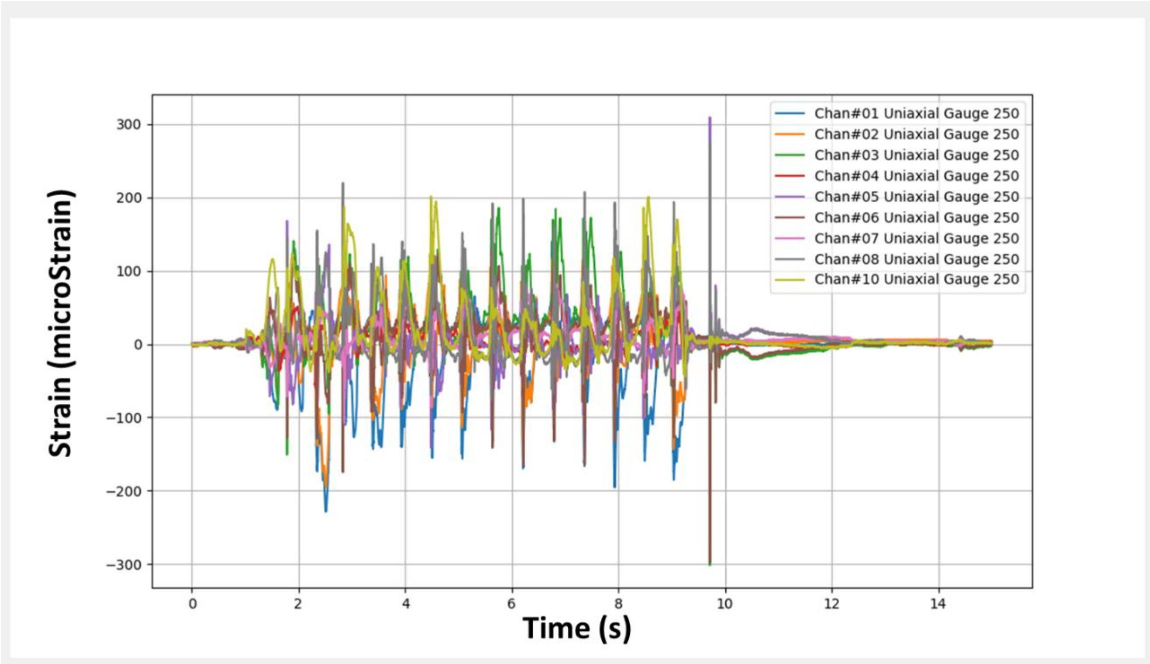

Figure 4-12 Typical Strain Traces from Test

4.8 The Pogo Stick: Post-Test

Once the strain data has been collected, it is processed to reconstruct the applied loading to the system. This is done by multiply the measured strain data times the correlation matrix extracted from the FEA model. The result will be a time history of loading scale factors for each of the applied loads to the Pogo Stick.

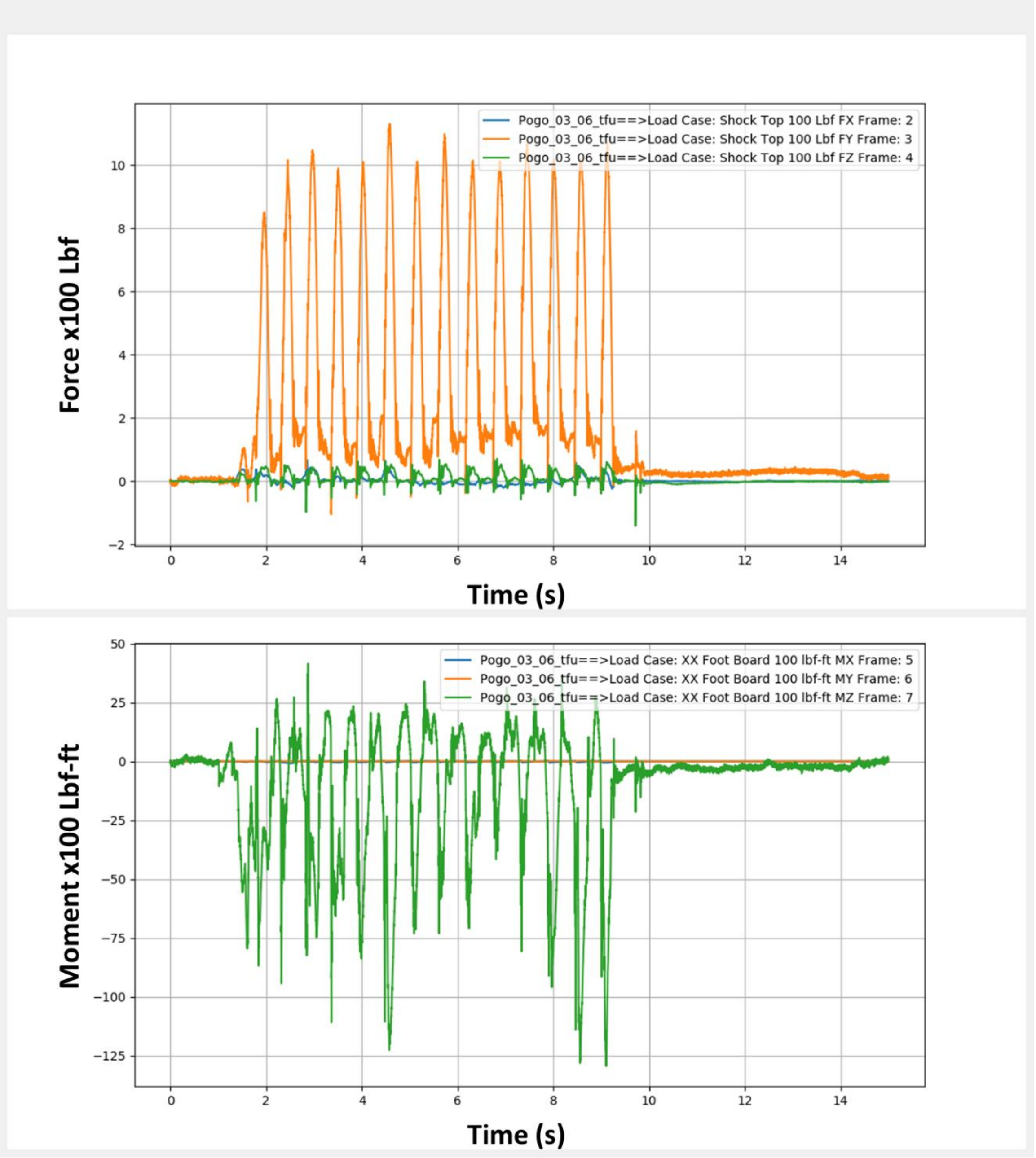

Figure 4-13 Reconstructed Loads

For this application, the True-Load/Post-Test software was used to perform this load reconstruction. In addition to the load reconstruction, several automatic post processing tasks are performed. This will produce an HTML report which contains plots of the reconstructed loads and a set of plots showing the measured strain and simulated strain from the reconstructed loads at the strain gauge locations in the FEA model. These measured / simulated strain plots are summarized in an overall plot of the simulated strain (blue) and the measured strain (green). In addition, there will be a cross plot of simulated vs measured strain. Ideally this would be a perfectly straight line on a 45 degree angle.

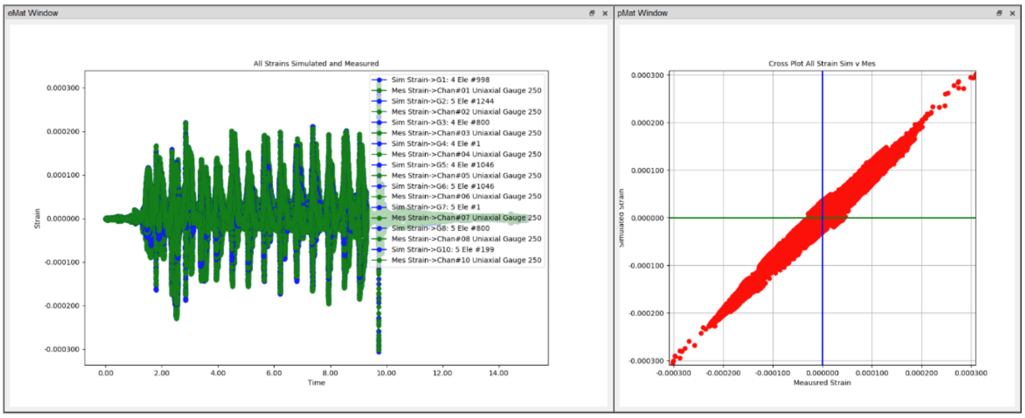

Figure 4-14 Overall Strain Correlation Plot

4.9 The Pogo Stick ODS

Once there is confidence in the reconstructed loads, detailed post processing of the FEA model may be performed. Having a complete time history of loads it is possible to construct operating deflection shapes of the entire scooter utilizing the time history of loading and the FEA model. Below is typical plot of frame from an operating deflection shape on the scooter.

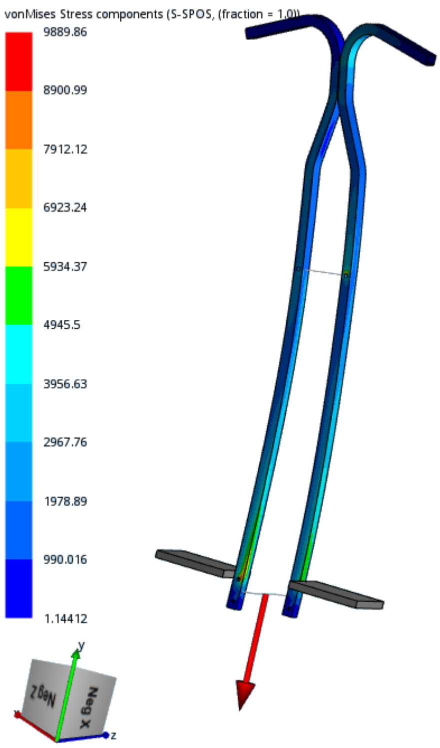

Figure 4-15 Typical Frame from a Reconstructed Operating Deflection Shape

5 Conclusion – Load Reconstruction

It has been shown in this paper that complex / nonlinear loading on a structure can be recovered at very high accuracy. The loading DOF were sufficiently complex (FX, FY, FZ spring, MX, MY, MZ at the foot pad support bar) to make this a non-trivial problem. If traditional load measurement techniques were to be deployed, the Pogo Stick would have been rendered inoperable.

With moderate skill and test plan processes, efficient placement of strain gauge can be placed on the structure to back calculate virtually any load conceived of by the FEA analyst. The cost for calculating these loads is two uniaxial strain gauges per loading DOF which is approximately $20. This is a highly cost effective and efficient process for determining complex loading on structures.

6 Rubber Fatigue: Endurica

The rubber tip of the pogo stick is an elastomer that deforms with nonlinear stress-strain behaviour under load. In order to track damage to the tip in real time, we split the analysis tasks into two categories: 1) calculations that are done once in a pre-step and then stored for later reuse, and 2) calculations that are done as part of the operating digital twin update process that executes each time digital twin status measurements (x, y and z loads vs. time) are made available from the True-Load reconstruction of load history. The analysis utilizes several commercial, off-the-shelf components: a nonlinear Finite Element solver (in this case MSC/Marc), the Endurica EIE interpolation engine, and the Endurica DT incremental fatigue solver. A custom-built software dashboard was also developed to automate the process of updating the pogo stick rubber tip digital twin and to provide a simple means to visualize the results at each update.

6.1 Pre-Step Calculations

6.1.1 Building the Endurica EIE Map

Because of rubber's nonlinear behaviour, the linear superposition of unit load cases is not a valid method for converting load history into strain history. Nor is it an option to run a full finite element analysis of the load history at each update, given that typical model run time is roughly an hour for only a few seconds of real time loading history. Instead, the Endurica EIE interpolation engine is used.

Endurica EIE uses a pre-computed, nonlinear map that connects possible loading states of the rubber tip, as specified by the x, y, and z force components acting on the tip, to corresponding strain states occurring in each element of the finite element model, as shown in Figure 6-1. EIE leverages the assumption that there is a unique, one-to-one correspondence between points in the 3 channel loading space and deformation states of the material. Since rubber is nonlinearly elastic, the assumption is generally accurate.

The nonlinear map is constructed by solving the finite element model for a series of load cases. A 5 x 3 x 5 cubic grid was used with limits of +/-300 N in the x and z directions and 0 to -10000 N in the y direction, a total of 75 distinct load cases. The rubber tip was assumed to follow Neo-Hookean behaviour with C_{10} = 5 MPa, corresponding roughly to 80 Shore A hardness. The finite element model included 35184 elements and 39335 nodes using the MSC/Marc solver. The FEA of the nonlinear map ran in 6959 seconds (nearly 2 hours). The 75 load cases computed are shown in Figure 6-2.

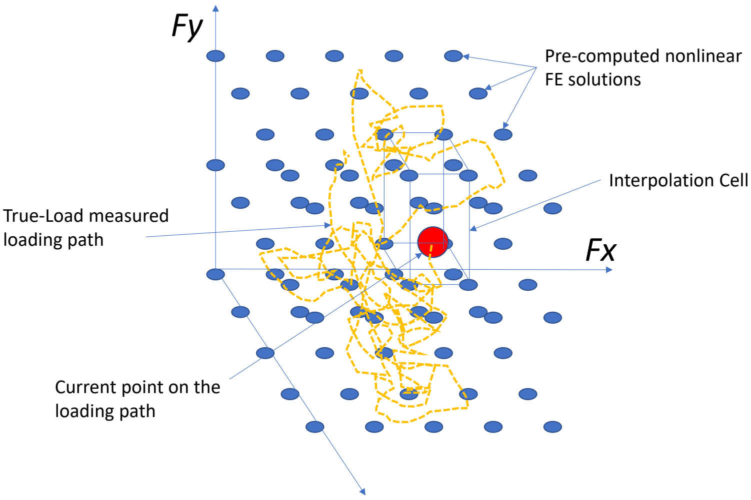

Figure 6-1 Endurica EIE interpolation scheme. Nonlinear finite element solutions are pre-computed for each map point. The pre-computed solutions are used to interpolate the strain components at each element for the current point on the loading path, based on the solutions at the vertices of the interpolation cell.

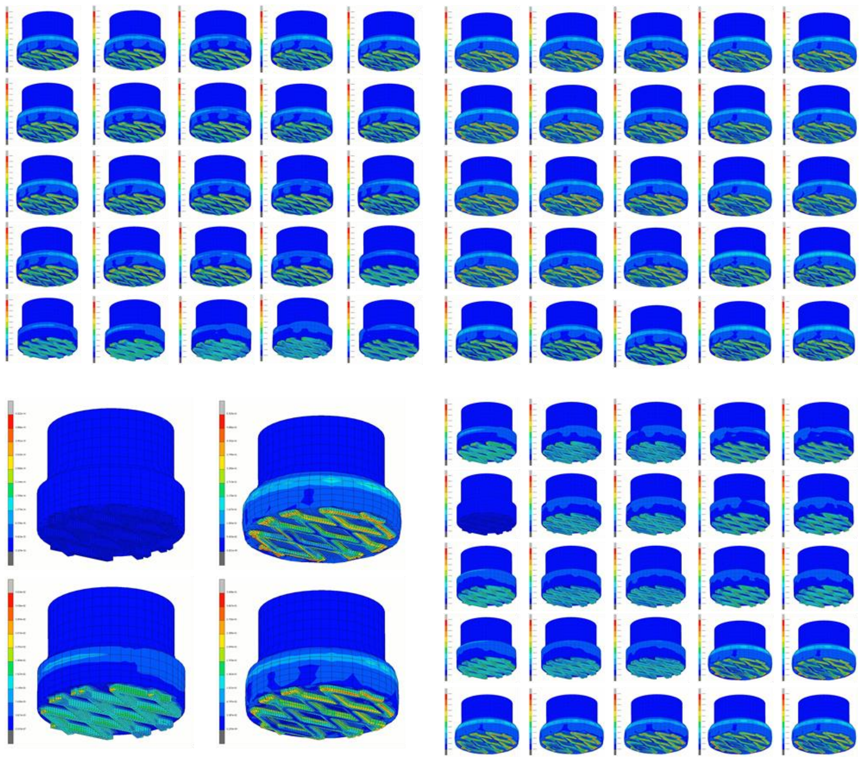

Figure 6-2 Pogo stick rubber tip finite element model results for the 75 cases comprising the map. Each case represents a unique combination of vertical and side loads. Contours show maximum principal strain.

6.1.2 Initializing Residual Life Calculation with Endurica CL

Damage is tracked via two metrics in the simulation. First, the Endurica fatigue solvers automatically track the growth of crack precursors within each finite element. Second, the Endurica DT incremental fatigue solver is used to track residual fatigue life. Residual fatigue life is defined as the number of repeats of a standard load case that would hypothetically be required to produce a 1 mm crack. The standard load case in this work is a single cycle from the unloaded state to a -1112 N vertical force (250 lbf, the weight limit for the pogo stick) with 0 side force.

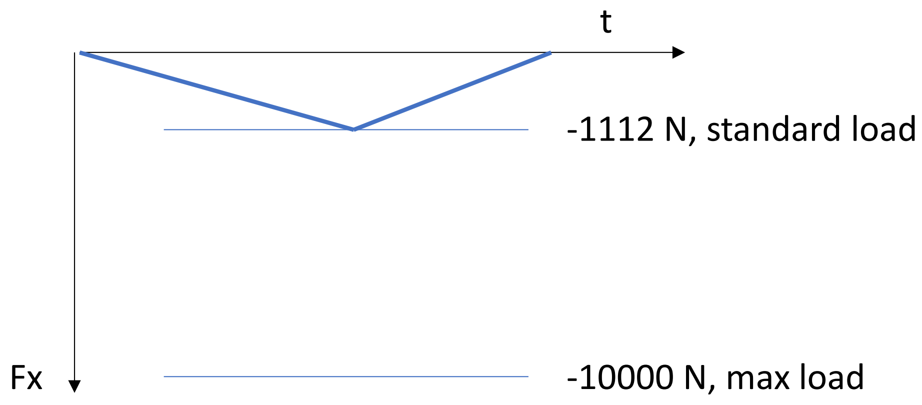

Figure 6-3 Pogo stick standard load case. Residual life is reported as repeats of this load case.

A call to the Endurica CL total fatigue solver, prior to the accumulation of any jumping cycles, is used to initialize the residual life. The following material definition is used:

```
**MATERIAL
mat=MATERIAL-1
elasticity_type=neohookean
c10=5.0 ! MPa
d1=0.0006667 ! 1/MPa
fatigue_type=thomas
size_pre=0.1 ! mm
size_eol=1.0 ! mm
tempcoef=0.0 ! 1/C
tempref=20 ! C
tcritical=12.0 ! kJ/m^2
rc=0.1 ! mm/cycle
f0=2.0
```

Endurica CL uses Critical Plane Analysis to determine the fatigue life for each element of the model. On each potential failure plane, the fatigue life is computed by integrating the crack growth rate law $r(T)$, where T is the energy release rate of the crack (Lake and Lindley 1964, Ait Bachir et al 2012, Li et al 2015). T and r are functions of the strain history ε_{mn}, the number of repeats N_f of the given duty cycle that are required to grow the crack precursor from original size c_0 to size c_f associated with end of life is given by

$$N_f = \int_{c_o}^{c_f} \frac{1}{r(T(\varepsilon_{mn}(N), \theta(N), c(N)))} dc$$

Equation 7: Total fatigue solver formulation.

The fatigue life on most critical plane in the shortest lived element for the rubber tip under the standard load case is N_f = 170824. The distribution of residual life for the standard case at time zero is shown in Figure 6-4. The compute time for the standard load case is less than 1 second running on 6 simultaneous cores.

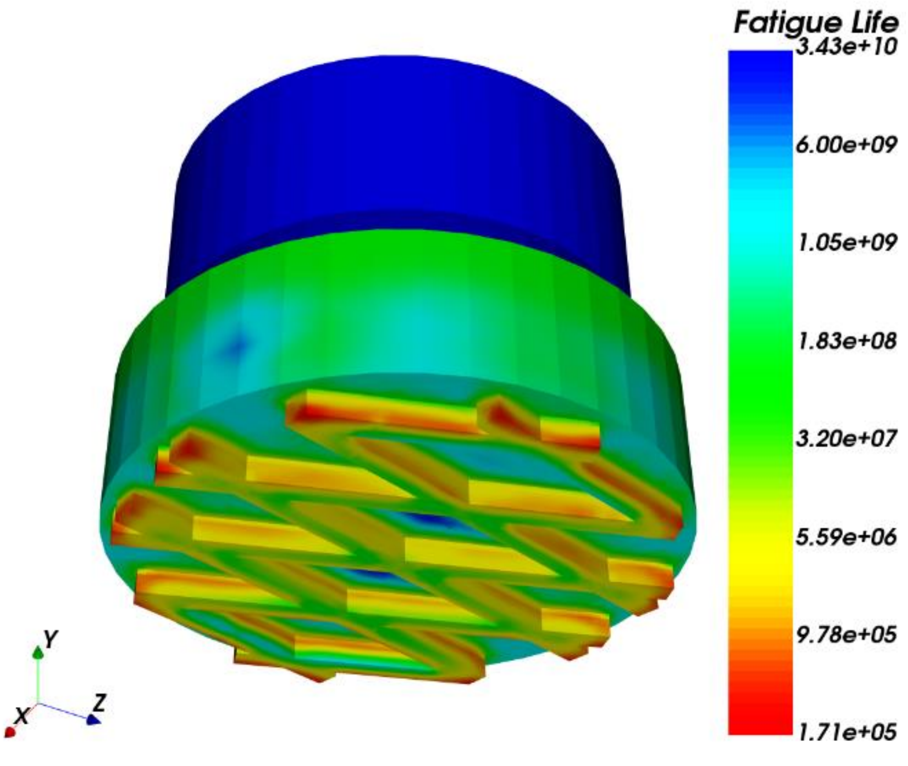

Figure 6-4 Initial distribution of residual fatigue life, given as repeats of the standard load case.

6.2 Updating Step Calculations

Once the map in EIE is set up and the residual life calculation initialized, updates to the model can be computed very efficiently. After receiving the most recent 3 channel loading history from True-Load, the process has the following steps: 1) generate strain history for all elements by interpolating the load history, 2) accrue damage to the rubber tip digital twin by evaluating the strain history with the DT incremental fatigue solver, and finally 3) display the results on a custom dashboard.

6.2.1 Load -> Strain history interpolation with Endurica EIE

In the present case, a 3 channel load history, typically with somewhere between 100 and 1000 time steps, is input to EIE to compute the history of 6 strain tensor components for 4582 elements in 1.6 seconds. Only elements on the surface of the tip are considered – it is known that cracking initiates from a free surface, and it saves considerable compute time to consider only those elements. 4 cores were used for the interpolation process. An example load input history is shown in Figure 6-5, along with interpolated results for the most critical element. Figure 6-6 shows the principal engineering strain history following interpolation. Figure 6-7 shows the cracking energy density and crack plane open/close state for the most critical element, numbered 35161.

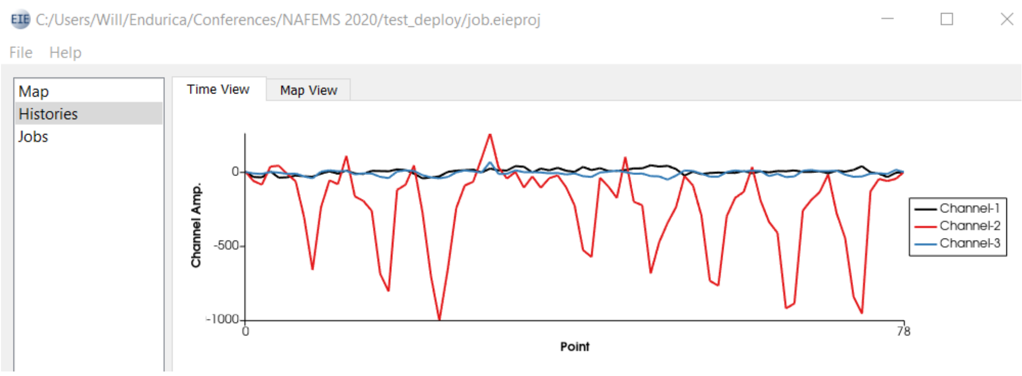

Figure 6-5 Typical history showing x, y and z loads experienced during a series of jumps.

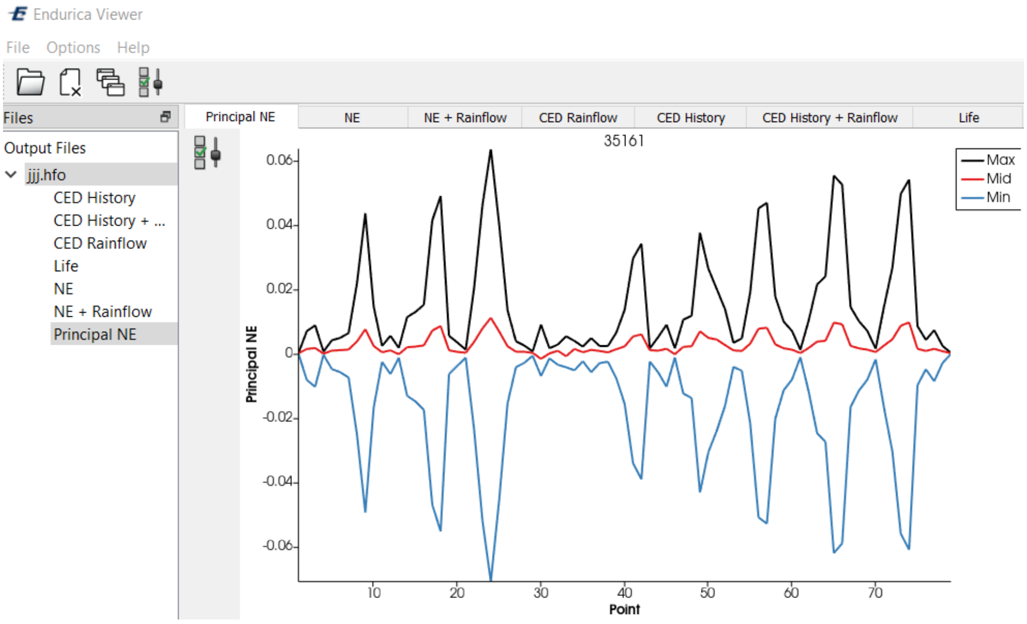

Figure 6-6 Maximum principal engineering strain history in most critical finite element as solved via the interpolation process.

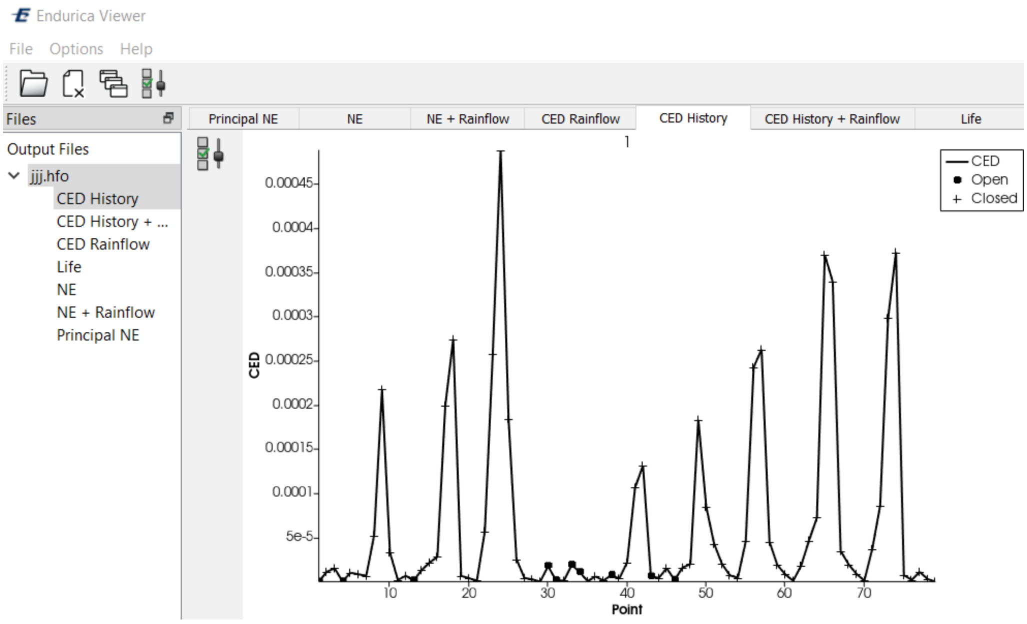

Figure 6-7 Cracking energy density history on the critical plane in the most critical finite element. The crack open/close state is indicated by the symbols.

6.2.2 Accrue Damage with Endurica DT

Once strain history is known for the surface elements of the rubber tip, the next step is to accrue the associated damage. This is accomplished using the Endurica DT incremental fatigue solver. The incremental solver is based on the following calculation (Mars et al 2018), which is made for each possible failure plane in each element. This formulation utilizes the same crack growth rate laws and input variables as used to initialize the residual life, but it instead integrates over cycles from time N_i to time N_{i+1}, rather than over crack size.

$$\Delta c_{i \to i+1, j, k} = \int_{N_i}^{N_{i+1}} r(T(\varepsilon_{mn}(N), \theta(N), c(N)))dN$$

Equation 8: Incremental fatigue solver formulation.

The result of the integration is the change of length $\Delta c_{i \to i+1, j, k}$ of a crack for each finite element *j* and each potential failure plane *k* of the model. The accumulated cracks lengths for each element are written to a file during the analysis, so that future additions of load history may begin at the point at which the prior increment left off. The basic incremental workflow for 3 successive periods is shown in Figure 6-8, and the resulting changes to crack growth are shown in Figure 6-9. These results were computing by repeating the load history from Figure 6-5 three times. In this case, each repeat of the history reduces the residual life by 3 repeats of the standard load case, as indicated in Figure 6-10.

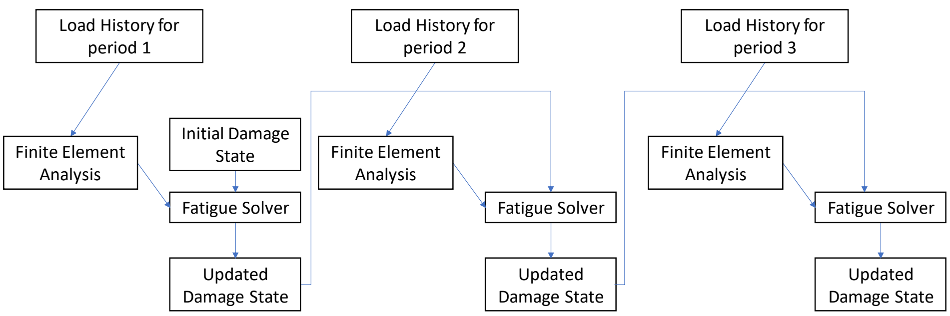

Figure 6-8 Incremental fatigue analysis workflow.

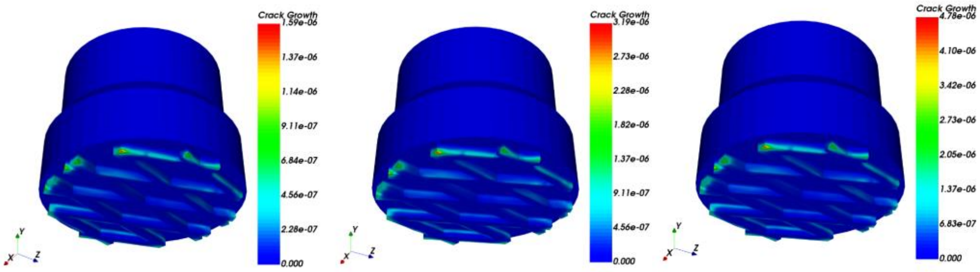

Figure 6-9 Crack precursor development over 3 update periods.

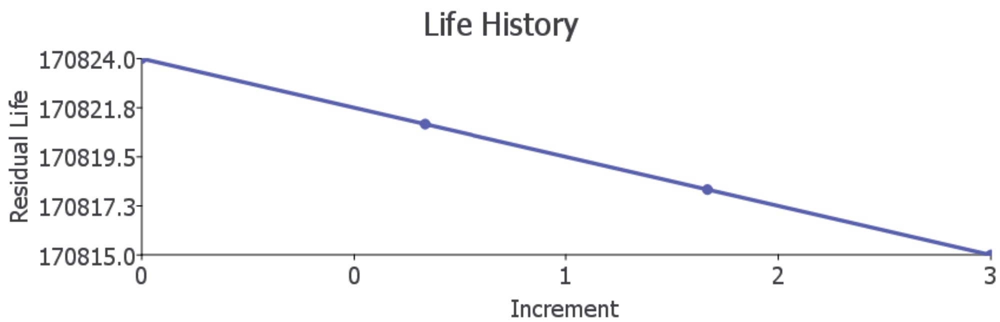

Figure 6-10 Development of residual life, measured in repeats of the standard load case, over 3 update periods.

6.2.3 Update and Visualize with Custom Visualization Dashboard

A custom dashboard for displaying the current state of the pogo stick digital twin was developed. The application manages the initialization and update processes describe above, and then plots the results following each update. The most recent value of the residual life is displayed at the top of the screen, with the change in residual life from the most recent update noted in parentheses. In the upper right hand side of the screen, there are indicator lights for each step of the update process, provided to demonstrate the relative computational load of each step. Two plots are provided on the left side of the screen. The topmost plot is the load history from all 3 channels from the most recent update. The bottommost plot is the history of the residual life over all prior updates. A contour plot is provided in the bottom right corner of the screen displaying either the residual life distribution (default) or the distribution of crack length change (if the checkbox is checked). New updates to the digital twin can be processed by hitting the Update button, and selecting a new input file with loads from the latest round of pogo stick jumps.

Figure 6-11 Dashboard application for managing and displaying digital twin state.

7 Example Results

The results from a series of jumping sessions are summarized below.

Update #	True-Load loads filename	Residual Life, repeats of standard case	Crack Growth, mm
Initialize	Standard load case	170824	0
1	pogoStickUnitLoads_v3-Pogo_03_01-D9-QSE-PV.csv	170821 (3)	1.59e-6
2	pogoStickUnitLoads_v3-Pogo_03_02-D9-QSE-PV.csv	170818 (3)	3.42e-6
3	pogoStickUnitLoads_v3-Pogo_03_03-D9-QSE-PV.csv	170812 (6)	6.72e-6
4	pogoStickUnitLoads_v3-Pogo_03_04-D9-QSE-PV.csv	170803 (9)	11.0e-6
5	pogoStickUnitLoads_v3-Pogo_03_05-D9-QSE-PV.csv	170801 (2)	12.4e-6
6	pogoStickUnitLoads_v3-Pogo_03_06-D9-QSE-PV.csv	170793 (8)	16.4e-6
7	pogoStickUnitLoads_v3-Pogo_03_07-D9-QSE-PV.csv	170789 (4)	18.6e-6
8	pogoStickUnitLoads_v3-Pogo_03_08-D9-QSE-PV.csv	170789 (0)	18.6e-6
9	pogoStickUnitLoads_v3-Pogo_03_09-Static-D9-QSE-PV.csv	170789 (0)	18.6e-6
10	history_trueload2.csv	169767 (1022)	84.1e-6
11	history_trueload3.csv	169170 (597)	132e-6
12	history_trueload4.csv	168995 (175)	144e-6
13	history_trueload2.csv	167973 (1022)	230e-6

8 Conclusions

Using commercial, off-the-shelf software on a small budget we have implemented and demonstrated a working digital twin for a pogo stick. We showed that the twin is capable of sensing and recording real-time loading history, and that the loads can be processed to accumulate and track damage, even for nonlinear components such as the rubber tip. The calculations execute with sufficient speed to provide a real-time dashboard application where current status of the structural health can be monitored.

The True-Load software provided load reconstruction based upon strain gauge readings, turning the pogo stick into its own multi-channel load transducer.

The Endurica EIE interpolation engine provided strain history for the finite element model under actual loads, and the Endurica DT incremental fatigue solver provided the damage accumulation function.

REFERENCES

References should be placed here and using the Harvard reference system.

[1] Ewins, D. J., 2000, Modal Testing: Theory, Practice, and Applications, Research Studies Press Ltd., Baldock, England.

[2] Hillary, B., and Ewins, D. J., 1984, “The Use of Strain Gages in Force Determination and Frequency Response Function,” Proceedings of the 2nd IMAC, Or- 391 lando, FL, pp. 627–634.

[3] Bernasconi, O., and Ewins, D. J., 1989, “Modal Strain Stress Fields,” J. Modal Anal., 4(2), pp. 68–76.

[4] Li, D. B., Zhuge, H., and Wang, B., 1989, “The Principles and Techniques of Experimental Strain Modal Analysis,” Proceedings of the 7th IMAC, Las Vegas, NV, pp. 1285–1289

[5] Tsang, W. F., 1990, “Use of Dynamic Strain Measurements for the Modeling of Structures,” Proceedings of the 8th IMAC, Kissimmee, FL, pp. 1246–1251.

[6] Yam, L. H., Leung, T. P., Li, D. B., and Xue, K. Z., 1996, “Theoretical and Experimental Study of Modal Strain Analysis,” J. Sound Vib., 191(2), pp. 397-398

[7] Sommerfeld, J. L., and Meyer, R. A., 1999, “Correlation and Accuracy of a Wheel Force Transducer as Developed and Tested on a Flat-Trac Tire Test Sys- 399 tem,” SAE Paper No. 1999-01-0938, Detroit, MI.

[8] Masroor, S. A., and Zachary, L. W., 1990, “Designing an All-Purpose Force Transducer,” Exp. Mech., 31(1), pp. 33–35.

[9] Dhighra, A. K, Hunter, T. G., and Gupta, D. K, 2013, “Load Recovery in Components Based on Dynamic Strain Measurements”, ASME Journal of Vibration and Acoustics, 135(5), VIB-12-1056; doi: 10.1115/1.4024384

[10] Szwedowicz, J., Senn, S. M., and Abhari, R. S., 2002, “Optimum Strain Gage Application to Bladed Assemblies,” ASME J. Turbomach., 124(4), pp. 606–613.

W Mars JD Suter, Incremental Critical Plane Method for Fatigue Analysis of Elastomers, CAASE19,

Barbash, Kevin P., and William V. Mars (2016). Critical Plane Analysis of Rubber Bushing Durability under Road Loads. No. 2016-01-0393. *SAE Technical Paper*.

Mars, William V., Matthew Castanier, David Ostberg, and William Bradford (2017). "Digital Twin for Tank Track Elastomers: Predicting Self-Heating And Durability." *NDIA Ground Vehicle Systems Engineering and Technology Symposium*.

Mars, William V., Jesse D. Suter, and Mark Bauman (2018). Computing Remaining Fatigue Life Under Incrementally Updated Loading Histories. No. 2018-01-0623. *SAE Technical Paper*.